Conformational and Substitution Effects on the Electron Distribution in a Series of Anthocyanidins

Laura Estévez and Ricardo A. Mosquera*

Departamento de Química Física, Facultade de Química, Universidade de Vigo, Lagoas-Marcosende s/n 36310-Vigo, Galicia, Spain

Received: May 8, 2009; Revised Manuscript Received: July 7, 2009

Density functional theory (DFT) and polarizable continuum solvation model (PCM) calculations have been applied to the study of the acid/base and prototropic equilibria of anthocyanidins. The results indicate that, excluding pelargonidin, the most favored neutral tautomers in solution are deprotonated at C4′. With the same exception, deprotonations at C5 and C4′ characterize the most stable anionic tautomers in solution. The equilibrium population of tautomers is mainly modified along the series by the substitution pattern on the B-ring. Electron densities, analyzed within the formalism of the quantum theory of atoms in molecules (QTAIM), indicate that the electron distribution of cations, neutral forms, and anions is not well described by the Lewis structures usually employed to represent them.

Introduction

Anthocyanins are a group of glycosilated flavonoids, hydroxylated and methoxylated derivatives of flavylium (2-phenyl-1-benzopyrilium) salts, which mainly contribute to the red, purple, and blue color in many fruits, vegetables, and grains.[1] Like all flavonoids, the backbone of its molecular structure consists of an aromatic ring (A-ring) bonded to a heterocyclic ring (C-ring) that contains oxygen, which is also bonded by a C−C bond to another aromatic ring (B-ring). They have six different aglycons or anthocyanidins, pelargonidin (Pg), cyanidin (Cy), delphinidin (Dp), peonidin (Pn), petunidin (Pt), and malvinidin (Mv). They are differentiated by the number and position of hydroxyl and methoxyl groups on their B-ring (Figure 1).[1,2] Their chromatic features are importantly affected by the hydroxylation/methoxylation pattern in the B ring. Thus, the color of anthocyanidins changes from red to blue as the number of hydroxyls increases, whereas the replacement of hydroxyls by methoxyl groups reverses the trend.[3] The color properties of anthocyanidins and being health-promoting disease-preventing dietary supplements make them particularly attractive candidates to replace artificial red or purple food colorants.[4] Thus, anthocyanidin colorants could be used in many solid foods such as extruded snacks and baked cakes as well as in drinks and beverages.[5] Nevertheless, so far, anthocyanidins have not been broadly used, because they are not as stable as synthetic dyes. In fact, it is known that the color of the same anthocyanidin also changes with the pH. That is because anthocyanidins experience prototropic equilibria and may exist in a variety of forms whose relative proportion is strongly dependent on pH. Thus, the red flavylium cation is dominant at very acidic pH (pH 1−3) and can be transformed into the purple-neutral form through proton transfer reactions. When the pH is between 6 and 7, it can be further converted into the blue-purple anions.[6,7]

Anthocyanins are more stable and soluble in aqueous solutions than anthocyanidins.[8] Therefore, anthocyanins are more common in nature, while their aglycones hardly exist as such in vivo. Nevertheless, their bioactivity is attributed to the aglycon but not to the sugar or other binding species.[9] Thus, the computational study of these compounds can be concentrated on that of the aglycons, which have been the subject of diverse quantum chemical studies. Nevertheless, most of these investigations were related exclusively to the cations[10,12] or carried out with semiempirical methods.[13] A recent paper[14] studies a set of anthocyanidins at a DFT level including the diverse species of the prototropic equilibria but it does not include the solvent effects in the calculations. For these reasons, in previous papers, we have reported an intensive DFT (Density Functional Theory) conformational study on pelargonidin,[15] the simplest anthocyanidin, and on delphinidin,[16] which displays the pyragallol moiety in the B-ring. From these works we conclude that there are different patterns in conformational behavior. Thus, the most stable tautomer of the neutral form of delphinidin is that deprotonated at C4′ but for neutral pelargonidin the most favored deprotonation takes place at C5. Furthermore, theoretical results obtained on isolated molecules can be compared to experiments only in a few cases, because most of the experiments are performed in liquid solutions. For this reason, in those works we have also performed calculations with the polarizable continuum model (PCM), first proposed by Miertuš, Scrocco, and Tomasi,[17] that has proven to be a reliable tool for the description of electrostatic solute−solvent interactions.[18] Thus, we observed some changes in the prototropic preferences of pelargonidin when the calculations were performed in aqueous solution, while these preferences remained unchanged for delphinidin.

We think that to determine which tautomers are significantly present in solution at a given pH and to clarify the effects of substitution on the prototropic equilibrium will be helpful to rationalize the chemical behavior of the diverse anthocyanidins. All this information is also valuable for developing new anthocyanidin structurally related food additives. This work aims to report which are the most stable tautomers and conformers of each anthocyanidin. It also looks for an interpretation of these preferences that could be useful for predicting the preferred tautomers and conformers for other combinations of substituents, as those present in synthetic derivatives. We also point to

* Corresponding author. E-mail: mosquera@uvigo.es.

10.1021/jp904298z CCC: $40.75
Published on Web 08/17/2009

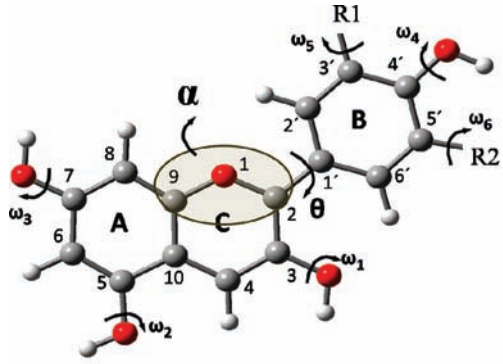

	R1	R2
Pg	H	H
Cy	OH	H
Dp	OH	OH
Pn	OCH_3	H
Pt	OCH_3	OH
Mv	OCH_3	OCH_3

Figure 1. General structure for the six anthocyanidins. Labeling scheme for the three rings (**A**, **B**, **C**), atom numbering, main dihedral angles ($\omega_1-\omega_6$ and θ), and α area entailing C2, O1, and C9 atoms are also shown.

provide a set of data useful to quantify the proportion of the diverse prototropic forms and conformers of anthocyanidins at a given pH.

Once the conformational and prototropic trends are known, our next goal is related to their electronic properties. In this context, we have two main objectives: (a) to describe the evolution experienced by the electron density along the prototropic equilibria; and (b) to discuss the reliability of classical resonance structures to describe the electron density, taking into account previously reported shortcomings detected for related compounds.[19] These tasks were done by applying the Quantum Theory of Atoms in Molecules, QTAIM, developed by Bader,[20] which has been extensively reviewed in the literature.[20−23]

Computational Details

In our conformational analysis we have considered all the conformations obtained by combining *a* (nearly antiperiplanar) and *s* (nearly synperiplanar) arrangements of ω_1, ω_2, and ω_3, whereas for the hydroxyls bonded to the B-ring ($\omega_4-\omega_6$), when it is possible (Figure 1), we have only considered those combinations that maximize the number of intramolecular hydrogen bonds (IHBs). As it was done in previous works, conformations of anthocyanidins are named by acronyms made by an italic capital letter indicating the concrete acid/base form considered (C = cation, N = neutral, A = anion) followed by a series of low case letters indicating approximated values of the main dihedral angles defining the orientation of the diverse hydroxyl or methoxyl groups. In this work we must also indicate the corresponding anthocyanidin using the nomenclature shown in Figure 1.

Initial conformations of the different forms of anthocyanidins (cation, neutral and anion) were fully optimized with the B3LYP[24] hybrid density functional with Gaussian03 package.[25] Because of the importance of π-electron delocalization in anthocyanidins, theoretical investigations require an accurate description of the electron density over the entire molecule to take into account all the possible electronic effects; therefore, we have used the 6-31++G** basis set. The inclusion of diffuse functions in the basis set can properly describe the long-range behavior of molecular orbitals associated with anionic systems. Vibrational frequencies were computed at the same level of theory for all the optimized structures with the aim to characterize them as minima and saddle points and to estimate zero point vibrational energies (ZPVEs). Solvent effects were computed using the polarizable continuum model, PCM.[26] Complete geometry optimizations were performed with PCM, taken all the gas phase conformers as initial geometries. The molecular Gibbs energy G of the solute embedded in a continuum medium is defined as the reversible work needed to create a cavity with a suitable shape in the medium, and to build up the molecule in this cavity, starting from noninteracting electrons and nuclei. The PCM model calculates the molecular free energy in solution as the sum over four terms:

$$G_{sol} = G_{ele} + G_{dis} + G_{rep} + G_{cav}$$

$$G_{ele} = E^0 + E_{pol}$$

These components represent the electrostatic (ele) and the nonelectrostatic contribution, the dispersion (dis), repulsion (rep), and the cavitation energy (cav), to the free energy. G_{ele} contains two terms: the electronic energy of the same molecular geometry in the gas phase, E^0, which differs from that of the optimized gas phase geometry, E^{GAS}, and that due to the electrostatic interactions with the solvent as modeled with PCM, E_{pol}. In this work, following the usual trend, ΔG_{sol} denotes the difference between G_{sol} values obtained for a certain rotamer and the most stable one along that series.

In the PCM method the solute are imbedded in a cavity of a continuum medium characterized by its dielectric constant. This cavity is created via a series of overlapping spheres centered on nuclei. The radii of the spheres are essential parameters of the method, for which several choices can be made. In this work we use the Simple United Atom Topological Model (UAO) set of solvation radii to build up the cavity by putting a sphere around each solute heavy atom: hydrogen atoms are enclosed in the sphere of the atom to which they are bonded.

Electron densities obtained at the same level, in the gas phase as well as in solution, were analyzed within the context of the QTAIM[20] using the AIMPAC package.[27] In this methodology, the electron density, $\rho(\mathbf{r})$, displays a (3,−1) singular point between every couple of nuclei connected by a bond, which is known as bond critical point (BCP) and whose coordinates will be denoted by $\mathbf{r}_c$. The set of points connecting the BCP and the two nuclei bonded is known as bond path. Among the properties computed at the BCP, the electron density, $\rho(\mathbf{r}_c)$, play a fundamental role to describe the interatomic interaction. So, higher values of $\rho(\mathbf{r}_c)$ indicate stronger bonds for the same pair of atoms.[28] The integration of the proper density function over the atomic basin, Ω, which is the space the atom occupies,[22,29] provides atomic properties. Three of them are of interest for our purposes here: electron atomic population, $N(\Omega)$, and its associated value of atomic charge, $q(\Omega)$, calculated by {1}, and the integrated value of the $L(\mathbf{r})$ function given by {2}, $L(\Omega)$,

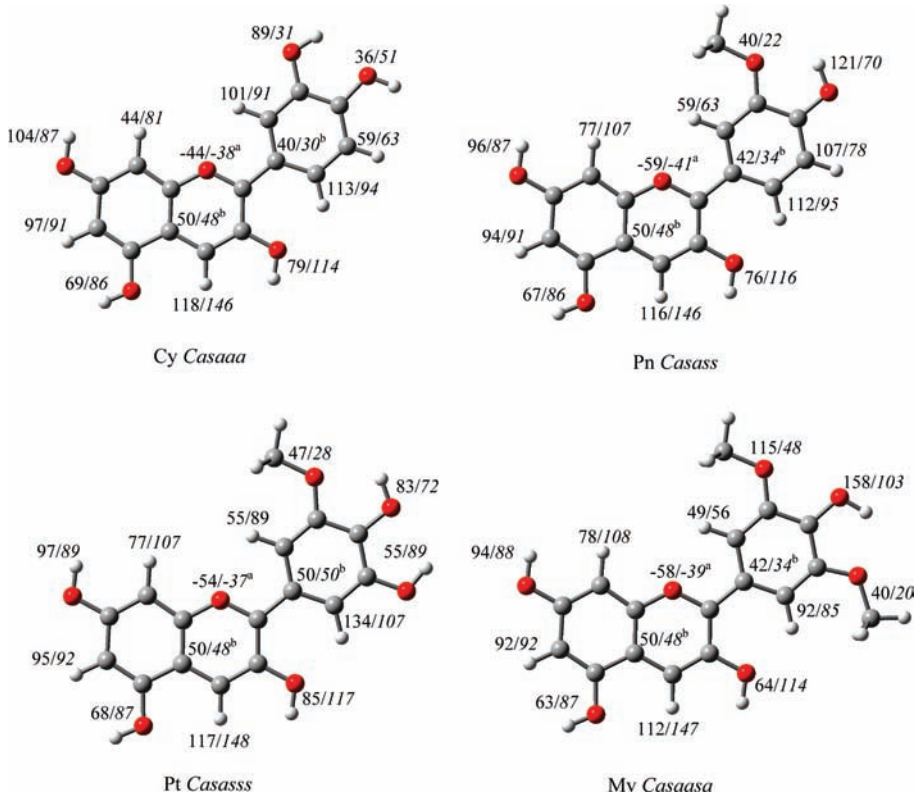

Figure 2. Most stable rotamer of the cationic form in the gas phase of Cy, Pn, Pt, and Mv. QTAIM charges (in au multiplied by 10^3) summed up into groups are shown for the gas phase and aqueous solution (in italics).

which should be zero for a perfectly determined basin. Integration errors $[N - \sum N(\Omega)]$ were always smaller (in absolute value) than 2×10^{-3} au. All atoms were integrated with $|L(\Omega)|^{20}$ less than 1×10^{-3} au.

$$q(\Omega) = Z_\Omega - N(\Omega) \quad (1)$$

$$L(\Omega) = \frac{-1}{4}\nabla^2\rho(\vec{r}) \quad (2)$$

Results and Discussion

Conformational Study. Our previous studies on pelargonidin[15] and delphinidin[16] have shown that the preferred orientation of the OH groups of anthocyanidins is largely influenced by the neighboring groups and by the geometry. These studies have also proved that the syn/anti disposition of the different OH groups gives rise to important differences in the energy sequence of conformers and tautomers. That is, the properties of these molecules are conditioned by the orientation of the substituents. Thus, knowing the preferred orientations of substituents is a prerequisite for searching relations between structure and activity. Then, we first focus on the geometrical characteristics obtained from the theoretical calculations. The conclusions inferred from our previous complete conformational analysis on pelargonidin[15] and delphinidin[16] in the gas phase and in solution are used as a reference for the other anthocyanidins. As in our previous papers, we report separately the results for cationic, neutral, and anionic forms.

Cationic Forms. The results of the optimization show that the antiperiplanar arrangement of ω_1 is the most favored one for all the cationic species and the conformer adopts a planar conformation, in which the dihedral angle between C and B rings, θ, is 0°. In contrast, the internal rotation around ω_1 to obtain an *s* arrangement, gives rise to a nonplanar conformer where θ departs from 0°. This agrees with previous studies[11] and is in line with the expected high repulsions between H6′ and H3.

The structures of the most stable rotamer of the cationic form of Cy, Pn, Pt, and Mv are shown in Figure 2. As observed for Pg and Dp, the most stable rotamer of the cationic form for Cy, in the gas phase, displays all the dihedral angles in the anti disposition, excluding the ω_2 dihedral angle (*Casaaa*). That is, all the OH groups in the B-ring prefer the anti disposition. Concerning ω_2, an imaginary frequency is observed when it is turned to anti. The same had been observed for Pg and Dp and is also true for most of the remaining compounds in this work (Table 1).

The above trend for the disposition of the OH groups of the B-ring is broken when the 3′-OH group is substituted by a methoxyl group as in Pn and Pt. Thus, the methoxyl group in the anti disposition gives rise to nonplanar structures where the ω_5 dihedral angle is 55.6° out of plane from the anti disposition, whereas the anti planar structure ($\omega_5 = 180°$) gives an imaginary frequency (about 65i cm^{-1}). Hence, we found that, in the most stable rotamer for the cationic form of Pn and Pt, the methoxyl group at 3′ position is in syn and these rotamers are completely planar. The energy differences between planar (syn) and nonplanar (anti) dispositions of ω_5 dihedral angle for Pn and Pt are, respectively, 26.3 and 22.3 kJ mol^{-1}, which points out the crucial effect of this group. We conclude that the most stable cationic forms, in the gas phase, of Pn and Pt are the rotamers *Casass* and *Casasss*, respectively (Table 1).

In Mv, where 3′and 5′ positions are substituted by methoxyl groups, we found that the most stable rotamer is that displaying, respectively, syn and anti dispositions for the 3′- and 5′-methoxyl groups. The 4′-OH group is also in anti to form an IHB with

TABLE 1: B3LYP/6-31++G Relative Energies (in kJ mol^{-1}) in the Gas Phase, ΔE_{gas}, and ΔG_{ele}, E_{pol} (in kcal mol^{-1}), and ΔG_{sol} Values (in kJ mol^{-1}; see Text) for the Different Rotamers of the Cation of the Six Anthocyanidins and Boltzmann Equilibrium Populations (at 298 K) in Solution, *N* (in %)**

		ΔE_{gas}	ΔG_{ele}	E_{pol}	ΔG_{sol}	*N*		″	ΔE_{gas}	ΔG_{ele}	E_{pol}	ΔG_{sol}	*N*
Pg	*Casaa*	0.0	0.0	−74.93	0.0	27.1	Pn	*Casass*	0.0	0.0	−70.84	0.0	49.8
	Casas	1.0	0.0	−75.40	0.0	27.2		*Cassss*	0.3	0.2	−71.31	0.2	46.8
	Caaaa	21.9	14.7	−79.09	15.2	0.1		*Casaaa*	26.3	8.6	−76.05	6.6	3.3
	Cssaa	8.0	10.5	−74.77	11.2	0.1							
Cy	*Casaaa*	0.0	0.6	−78.26	0.6	43.9	Pt	*Casasss*	0.0	0.0	−74.59	0.0	53.8
	Casass	3.3	0.0	−79.90	0.0	55.7		*Casssss*	0.4	0.7	−75.06	0.6	42.3
	Caaaaa	24.1	13.9	−81.23	12.3	0.4		*Casaaaa*	22.3	8.3	−80.02	6.5	3.9
	Csaaaa	7.4	11.4	−72.07									
Dp	*Casaaaa*	0.0	0.0	−81.76	0.0	27.2	Mv	*Casaasa*	0.0	0.0	−71.96	0.0	84.7
	Casasss	3.7	0.0	−83.28	0.0	26.9		*Casaaaa*	5.7	6.6	−71.68	5.2	10.4
	Caaaaaa	24.9	14.8	−84.10	16.3	0.0		*Casasss*	8.4	7.8	−72.10	7.1	4.9
	Cssaaaa	8.6	12.2	−80.91	13.6	0.0		*Cssaaaa*	13.7				

TABLE 2: Selected Bond Lengths (in Å) for the Most Stable Rotamer of the Cationic, Neutral, and Anionic Form of the Six Anthocyanidins

	Pg Casaa	*Cy Casaaa*	*Dp Casaaaa*	*Pn Casass*	*Pt Casasss*	*Mv Casaasa*
C4′−O4′	1.343	1.353	1.347	1.336	1.346	1.333
C2−C1′	1.440	1.443	1.442	1.437	1.440	1.435
C2−O1	1.351	1.350	1.351	1.354	1.353	1.355
C3−O3	1.358	1.358	1.360	1.358	1.356	1.361
C5−O5	1.352	1.352	1.352	1.352	1.352	1.353
C2−C3	1.422	1.420	1.421	1.425	1.424	1.426
	Pg Naxsa	*Cy Nasaxa*	*Dp Nasaxas*	*Pn Naxsss*	*Pt Naxssss*	*Mv Naxsasa*
C4′−O4′	1.364	1.249	1.255	1.357	1.366	1.355
C2−C1′	1.462	1.397	1.400	1.461	1.463	1.461
C2−O1	1.366	1.379	1.378	1.367	1.367	1.366
C3−O3	1.374	1.367	1.365	1.373	1.371	1.376
C5−O5	1.245	1.367	1.366	1.245	1.245	1.246
C2−C3	1.385	1.448	1.447	1.386	1.386	1.387
	Pg Aaxsx	*Cy Aaxsxa*	*Dp Aaxsxas*	*Pn Aasass*	*Pt Aaxsxsa*	*Mv Axxsasa*
C4′−O4′	1.255	1.267	1.277	1.250	1.278	1.373
C2−C1′	1.418	1.422	1.425	1.416	1.431	1.450
C2−O1	1.371	1.370	1.370	1.373	1.365	1.376
C3−O3	1.384	1.384	1.382	1.384	1.368	1.274
C5−O5	1.260	1.259	1.259	1.260	1.278	1.254
C2−C3	1.423	1.420	1.418	1.424	1.418	1.433

O5′-CH_3. Thus, the most stable cation of Mv is the rotamer *Casaasa*, which differs in energy with rotamer *Casassa* (in which the 4′-OH group forms an IHB with the O3′-CH_3 group) by less than 4.0 kJ mol^{-1}.

As far as geometries are concerned, bond lengths and bond angles are scarcely affected by substituent changes when they are compared with those in Pg. In fact, the largest variations observed for bond lengths in the carbon backbone are found for Cy in C4′−C5′ (0.009 Å), Dp in C1′−C2′, Pn in C3′−C4′ (0.016 Å), Pt in C5′−C6′, C2′−C3′, and C3′−C4′ (0.005 Å), and Mv in C3′−C4′ (0.009 Å). The C4′−O4′ bond length seems to be affected by the substituents at the ortho position. Thus, it is reduced by 0.011 and 0.007 Å in Mv and Pn, respectively, increased by 0.009 Å in Cy and by 0.003 Å in Dp and Pt (always with regard to Pg). Moreover, the finding that the C2−C1′ bond length (Table 2) is significantly shorter than that of a C−C single bond (1.54 Å) allows us to conclude that delocalization in the AC system is extended to the B-ring in all six anthocyanidins. The different substitution on the B-ring and the conformational preferences of the substituents produces significant differences among the bond angles of this ring (Supporting Information). On the contrary, the largest variation observed for the bond angles in the AC system is less than 1.1°.

All the cations display an O3···H6′−C6′ IHB, which is detected as a bond path in the QTAIM electron density analysis. As previously reported for Pg[15] and Dp,[16] this is a *blue-shifted* IHB. The largest blue shift is observed for the most stable rotamer of Mv cation, *Casaasa*, which presents the highest C6′−H6′ stretching, $\upsilon_{(C6'-H6')}$ (3306.0 cm^{-1}), and the shortest C6′−H6′ bond length, $r_{(C6'-H6')}$ (1.077 Å; Supporting Information). Some differences in the characteristics of these IHB can be observed with the conformational changes.[30] For contrast, there are not significant changes between rotamers in the other vibrational frequencies (data not shown). Properties at the IHB BCP also show that Mv has the strongest O3···H6′−C6′ IHB, for example, it has the largest ρ_b. Other IHBs, between 4′-OH and the adjacent 3′ or 5′ methoxyl group, are found in Pt, Pn, and Mv (Supporting Information). Finally, no bond path was detected between adjacent OH groups, cathecol moiety, as previously reported in several cases.[31]

Main energetic trends among the rotamers are retained on going from the gas phase to the water solution. We just notice the well-known decrease of energetic gaps (Table 1), whose origin has been discussed elsewhere.[32] We also notice some important variations of the polarization energy, E_{pol}, which could indicate that certain orientations let the solvent interact more

TABLE 3: B3LYP/6-31++G Relative Energies (in kJ mol^{-1}) for the Most Stable Rotamers of the Most Relevant Tautomers for the Six Anthocyanidins in the Gas Phase and *in Solution*[a]**

	neutral Forms						anion Forms					
	tautomer (rotamer)	ΔE_{gas}	ΔG_{ele}	E_{pol}	ΔG_{sol}	N	tautomer (rotamer)	ΔE_{gas}	ΔG_{ele}	E_{pol}	ΔG_{sol}	N
Pg	**N5** (*Naxsa*)	0.0	0.5	−42.81	0.7	20.3	**A54′** (*Asxsx*)	0.0	8.8	−74.07	8.7	0.7
	N3 (*Nxsaa*)	6.0	2.4	−44.40	2.7	8.8	**A54′** (*Aaxsx*)	2.0	0.6	−75.78	0.2	12.3
	N7 (*Nasxs*)	6.1	0.0	−45.21	0.0	26.2	**A35** (*Axxsa*)	10.9	0.0	−80.03	0.0	13.5
	N4′ (*Nasax*)	17.3	4.1	−51.88	4.6	4.1	**A74′** (*Aasxx*)	13.4	2.2	−81.17	1.7	6.8
Cy	**N4′** (*Nasaxa*)	0.0	0.0	−49.26	0.0	94.9	**A54′** (*Asxsxa*)	0.0	8.4	−72.45	9.0	1.7
	N5 (*Naxsss*)	11.0	10.0	−46.22	10.2	1.5	**A54′** (*Aaxsxa*)	3.4	0.0	−74.03	0.0	66.8
	N7 (*Nasxss*)	17.0	9.6	−49.83	9.7	1.9	**A34′** (*Axxsss*)	8.7	11.0	−74.78	11.5	0.6
	N3 (*Nxsaaa*)	19.5	12.7	−48.52	13.0	0.5	**A74′** (*Axxsaa*)	15.7	2.1	−79.73	1.9	30.8
	N3′ (*Nasasx*)	53.3	29.7	−59.26	29.5	0.0	**A35** (*Nxxsss*)	39.6	13.1	−83.85	13.5	0.3
Dp	**N4′** (*Nasaxas*)	0.0	0.0	−49.31	0.0	53.6	**A54′** (*Asxsxas*)	0.0	9.6	−62.23	10.4	0.5
	N5 (*Naxsaaa*)	25.2	19.2	−49.93	19.3	0.0	**A54′** (*Aaxsxas*)	6.2	0.0	−74.27	0.0	34.4
	N3 (*Nxsaaaa*)	25.9	20.4	−48.90	20.5	0.0	**A74′** (*Aasxxas*)	17.7	1.7	−79.63	1.5	18.7
	N7 (*Nasxsss*)	32.8	18.4	−53.39	18.2	0.0	**A34′** (*Axsaxas*)	26.3	1.7	−83.67	1.8	16.6
	N3′ (*Nasasxs*)	68.2	39.4	−62.45	39.2	0.0	**A35** (*Axxsaaa*)	53.1	20.8	−84.37	20.9	0.0
	N5′ (*Nasaaax*)	75.9	42.6	−64.71	42.4	0.0	**A3′5′** (*Aasssxx*)	198.9	78.1	−132.09	77.5	0.0
Pn	**N5** (*Naxsss*)	0.0	0.6	−38.44	1.2	22.7	**A35** (*Axxsss*)	0.0	2.6	−76.73	3.3	14.5
	N7 (*Nasxss*)	5.7	0.2	−42.20	0.6	29.1	**A54′** (*Aaxsxa*)	4.2	8.1	−75.13	6.7	3.7
	N3 (*Nxsass*)	9.9	3.4	−41.88	4.0	7.5	**A54′** (*Aaxsxs*)	6.7	0.0	−78.77	0.0	54.7
	N5 (*Naxsaa*)	25.3	11.8	−44.34	10.4	0.5	**A74′** (*Nasxxa*)	16.2	10.2	−80.65	8.6	1.7
	N4′ (*Nasaxs*)	27.6	0.0	−53.61	0.0	37.3	**A74′** (*Nasxxs*)	17.7	2.2	−83.80	2.0	24.3
	N4′ (*Nasaxa*)	29.2	9.5	−50.65	8.0	1.5	**A35** (*Axxsaa*)	22.8	11.0	−81.24	9.8	1.1
Pt	**N5** (*Naxssss*)	0.0	12.0	−42.32	12.5	0.6	**A54′** (*Aaxsxas*)	0.0	7.0	−73.98	5.8	5.9
	N4′ (*Nasaxss*)	5.0	0.0	−52.13	0.0	93.4	**A54′** (*Aaxsxss*)	3.1	0.0	−77.27	0.0	60.6
	N7 (*Nasxsss*)	5.5	11.3	−45.95	11.6	0.9	**A74′** (*Aasxxas*)	11.4	8.8	−79.28	7.4	3.1
	N4′ (*Nasaxas*)	6.5	8.3	−49.60	7.0	5.5	**A74′** (*Aasxxss*)	13.4	1.9	−82.01	1.7	30.2
	N3 (*Nxsasss*)	12.7	14.2	−47.56	14.6	0.3	**A35** (*Aaxsxss*)	25.1	13.0	−82.59	13.5	0.3
Mv	**N5** (*Naxsasa*)	0.0	4.9	−39.71	5.4	4.8	**A35** (*Axxsasa*)	0.0	3.6	−75.04	4.0	13.7
	N3 (*Nxasasa*)	3.1	17.6	−36.50	18.4	0.0	**A54′** (*Aasaxsa*)	16.2	0.0	−82.38	0.0	69.1
	N7 (*Nasxasa*)	6.9	4.5	−44.11	4.8	6.0	**A35** (*Axxssss*)	12.9	7.4	−78.53	10.7	0.9
	N4′ (*Nasaxsa*)	24.8	0.0	−55.70	0.0	42.2	**A74′** (*Aasxxsa*)	27.1	2.1	−87.52	1.9	24.3

[a] Polarization energy, E_{pol} (in kcal mol^{-1}), and Boltzmann equilibrium populations in solution (at 298 K), N (in %).

strongly with polar groups of the molecule; that is, those groups are more accessible. Thus, for example, E_{pol} is higher in the rotamer *Pn Casaaa* than in the *Pn Casass* by almost 25 kJ mol^{-1}. In general, E_{pol} is substantially larger in charged species than in neutral ones (Tables 1 and 3).

The most important effect of solvation on the geometries is the lengthening of the C−O and the O−H bonds, while the C−C backbone bonds are reorganized experiencing a sort of equalization with regard to the gas phase structure, lengthening the shortest and shrinking the longest ones with regard to those in the gas phase. The most significant enlargements in the C−C bond lengths are found at the C2−C1′ and C2−C3, but they are still shorter than a C−C single bond. We also notice that O3···H6′−C6′ IHB distance become longer in solution, accompanied by a decrease of the corresponding ρ_b values (Supporting Information). This indicates that the IHB interaction becomes less important in water solution, where the molecule may adopt other structure where ion−dipole intermolecular interactions dominate. The bond path associated to the H4′···OCH$_3$ IHBs commented for the gas phase is not detected for PCM results (see ref 16 for more detail). Bearing in mind the limited accuracy of PCM vibrational frequencies,[33] we are not discussing the effects of solution on *blue-shifted* IHBs.

Neutral Forms. As each anthocyanidin has several OH groups, we can distinguish several different neutral tautomers (**N**), which henceforth will be named by the atom attached to the carbonyl oxygen. Thus, we can obtain upon deprotonation four neutral tautomers, for Pg, Pn, and Mv, five for Cy and Pt, and six for Dp. Every one of them appears as a set of rotamers.

The optimized equilibrium geometries of all the neutral species, studied here, arising from parent cationic forms by removing a H$^+$ when raising the pH, are planar. Depending on the substitution degree of the B-ring, **N4′** or **N5** tautomers are found as the most stable ones (Figure 3). It has to be stressed that the values of ω_3 and ω_5 dihedral angles in these tautomers alter the energy more than the prototropic change. Thus, molecular energies of their rotamers are interspersed and we can say that ω_3 and ω_5 play a crucial role to determine the most stable form of neutral anthocyanidins. The very high relative energies of **N3′** and **N5′** found in Dp lead us to exclude these tautomers from our calculations in the remaining compounds. Because of the lack of general rules, we are describing the main trends of prototropic and conformational equilibria for each neutral anthocyanidin not previously reported.

Cyanidin. The most stable tautomer in the gas phase is obtained upon deprotonation at 4′-OH (**N4′**), and its most stable rotamer is *Nasaxa*. The next tautomer, **N5**, is 11.0 kJ mol^{-1} above after ZPVE corrections (*Naxsss* rotamer) and should not be observable in the gas phase equilibrium mixture. PCM optimizations also point to the **N4′** tautomer as the most stable one. There is only a slight decrease of relative energies of tautomers with regard to the gas phase (Table 3). This also supports that IHB interaction (which stabilizes the most stable conformer) becomes less important in water than in gas phase. For instance, the relative energy of *Nasaxs*, where there is no O4′···H3′ IHB bond path, goes down from 41.0 kJ mol^{-1} in the gas phase to only 10.7 kJ mol^{-1} in solution. Overall, we remark the influence of ω_5 on the relative energies among tautomers in both phases.

Peonidin. The most stable tautomer is that obtained upon deprotonation at 5-OH (**N5**), *Naxsss* being the most stable rotamer in the gas phase. It is noticeable the higher relative

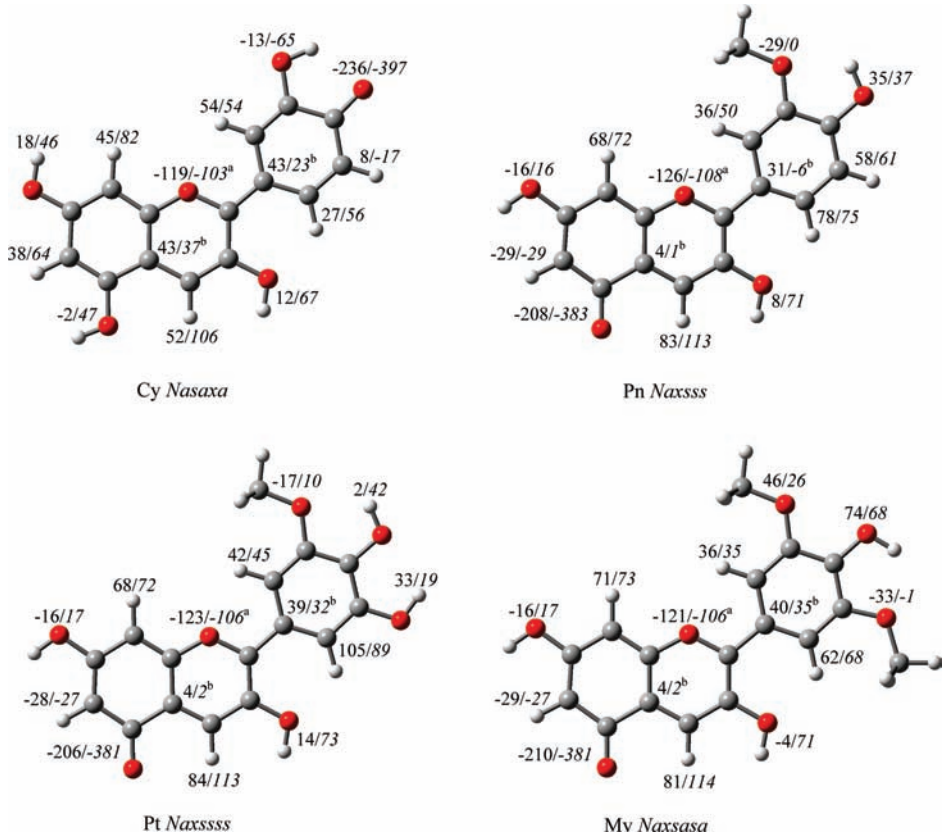

Figure 3. Most stable rotamer for the most stable tautomer of the neutral form of Cy, Pn, Pt, and Mv in the gas phase. QTAIM charges (in au multiplied by 10^3) summed up into groups are shown for the gas phase and aqueous solution (in italics).

energy of the other rotamer of **N5** tautomer, *Naxsaa* (whose ω_5 dihedral angle is not in the plane of the molecule): more than 25.3 kJ mol^{-1} after ZPVE corrections. The most stable rotamer of **N4′** is *Nasaxs* (27.6 kJ mol^{-1} above) where there is no ortho OH group in the B-ring to form the IHB. PCM calculations narrow and also alter the relative energies between tautomers, being **N4′** (*Nasaxs*) the most stable tautomer (Table 3).

Petunidin. The most stable tautomer is that obtained by deprotonating its 5-OH (**N5**) and its most stable rotamer is *Naxssss*. The *Nasaxss* rotamer (**N4′** tautomer) is only 5.0 kJ mol^{-1} above the minimum, even taking into account that this **N4′** displays an O4′···H5′ IHB. We also found in the conformational analysis that the other rotamer of **N5**, *Naxass*, is 9.0 kJ mol^{-1} above the minimum and 4.0 kJ mol^{-1} above the **N4′**, pointing out the significant effect of this dihedral angle, ω_3, in the prototropic equilibrium in the gas phase. **N4′** is found as the most stable in aqueous solution by almost 12 kJ mol^{-1}. This is explainable when looking at polarization energies and dipoles in aqueous solution.

Malvinidin. The most stable tautomer is that obtained upon deprotonation at 5-OH (**N5**) and the planar structure *Naxsasa* is the most stable rotamer in the gas phase. Other planar rotamers, *Nxasasa*, *Nasxasa*, and *Nasaxsa*, representing **N3**, **N7**, and **N4′** tautomers, are found, respectively, at 3.1, 6.9, and 24.8 kJ mol^{-1} above the global minimum. The most relevant fact is the relatively low energy of the **N3** tautomer in spite of the impossibility to draw an isovalent Lewis structure with the typical quinonoidal structure, as it has already been noticed by Rastelli et al.[13] This will be discussed below by using QTAIM atomic charges, which will be compared with those of the other neutral forms where the uncharged Lewis structure can be written. PCM results alter the stability sequence obtained for the gas phase. Hence, we observe that the most stable rotamer is *Nasaxsa* (**N4′** tautomer) followed by *Nasxasa* at 4.5 kJ mol^{-1} (**N7**), *Naxsasa* (**N5**) at 4.9 kJ mol^{-1}, and *Nxassaa* (**N3**) at 17.6 kJ mol^{-1}. This order must be explained by looking at the polarization energy (Table 3), which is higher in *Nasaxsa* than in *Naxsasa* (almost 67.0 kJ mol^{-1}). This makes up for the E^0 term, which favors the **N5** tautomer, providing G_{sol} values that favor **N4′**. The high differences in the polarization energy can be related to the high differences between dipoles (21.50 D in **N4′** and 6.82 D in **N5**).

All the planar rotamers of all neutral anthocyanidins studied in this work display (as commented above for the cations) the O3···H6′−C6′ IHB (detected as a QTAIM bond path) in both phases. In the gas phase, this IHB is still *blue-shifted* in the rotamers of **N3**. Thus, (a) the average value for $\upsilon_{(C6'-H6')}$ along **N3** rotamers is 3226.3 cm^{-1}, whereas it is 3276.7 cm^{-1}, in average, for the remaining tautomers; (b) the C6′−H6′ bond lengths are, in average, 1.083 and 1.079 Å, respectively. We also observe the following trends for this IHB: (i) Deprotonation affects it, displaying shorter O3···H6′ bond lengths in **N3** and **N4′** (0.06 and 0.01 Å, respectively) and larger ρ_b values than in the corresponding cation, contrasting with longer O3···H6′ bond lengths in **N5** and **N7** (0.03 Å) and smaller ρ_b values with regard to the corresponding cation (Supporting Information); (ii) This interaction seems to be stronger in the gas phase (interatomic distances increase in solution: 0.068 Å for **N3** and 0.015 Å for the remainders, and ρ_b values decrease slightly).

Other IHBs involving the deprotonated oxygen O4′ (**N4′** tautomers) and the adjacent hydroxyl group, as in Cy and Dp (interatomic distances: 2.019−2.134 Å and ρ_b at the H3′···O4′ and H5′···O4′; BCPs: 20.9 10^{-3} to 26.3 10^{-3} au); or H4′ and the adjacent methoxyl groups in Pt, Pn, and Mv (interatomic distances: 2.094−2.150 Å; and ρ_b: 17.9 10^{-3} to 20.2 10^{-3} au) are detected as a bond path in the gas phase.

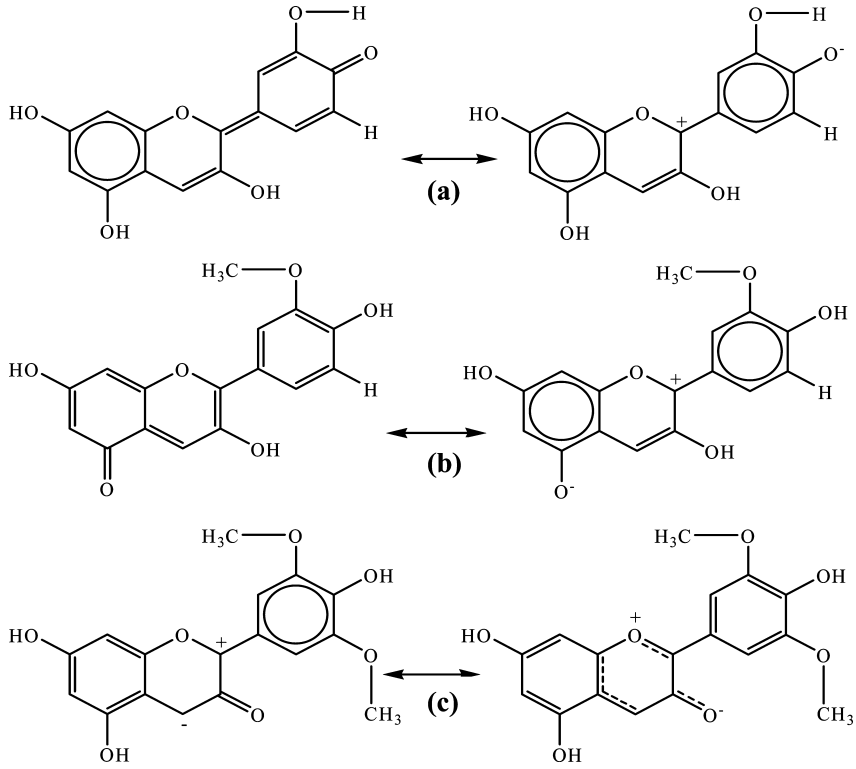

Figure 4. Some resonance structures for **N4′** (a) and **N5** (b) neutral forms of anthocyanidins. Other enolate resonance structures (not shown) place the positive charge on O1, C4, C7, C9, C2′, and C6′. **N3** resonance forms, where an uncharged Lewis structure cannot be drawn (c), are also shown.

Deprotonation gives rise to variations in the bond lengths (with regard to the cationic form) of the C−C backbone. The largest variations are displayed up to three bonds from the deprotonation site, although the characteristic resonance trend of alternant lengthening/shortening of bonds can be detected further. Thus, in the **N4′** tautomers we recognize in the B-ring three "short" bonds (C−O and the two C−C bonds parallel to the C−O axis) and four "long" C−C bonds, in agreement with the commonly written quinonoidal resonance structure with a formal C4′=O4′ double bond (Figure 4). The similar alternant lengthening/shortening trend is found when the deprotonation site is 5-OH or 7-OH (**N5** and **N7** tautomers). Nevertheless, this is not true for the **N3** tautomer, where the formal C3=O3 double bond would entail a nonisovalent Lewis structure (Figure 4, see below).

Comparing solution and gas phase geometries of the neutral species, we observe again that PCM makes some equalization of the C−C bond lengths, lengthening the shortest ones, and shrinking the longest ones. This equalization is especially intense in two cases: (i) in the B-ring of the **N4′** tautomers; and (ii) in the A-ring of the **N5** and **N7** tautomers. Furthermore, PCM lengthens the deprotonated C−O bonds, whereas in the remaining hydroxyls the C−O bonds shrinks while the O−H also lengths. Overall, according to PCM geometrical parameters, the quinonoidal structures become negligible and we could draw C4′−O4′, C5−O5, or C7−O7 single bonds for the corresponding tautomers.

Anionic Forms. Neutral forms are transformed into anions upon deprotonation of another hydroxyl in basic media. Their tautomers are named indicating the atoms attached to the two dehydroxylated oxygens after a capital **A**. Rotamers are named as in previous forms. **A54′** tautomer is the most stable anion in the gas phase for Pg, Cy, Dp, and Pt, while Pn and Mv prefer the planar **A35** anion (Table 3). The energetic trends among anions are almost retained on going from the gas phase to the aqueous solution but gaps among relative energies become smaller. **A54′** is the most stable tautomer of the anion forms for all the anthocyanidins, except for Pg, which changes in favor of **A35** by only 0.2 kJ mol^{-1}, while Mv changes its preferences for **A54′** over **A35** by 4.0 kJ mol^{-1}. The general reduction in the relative energies obtained with PCM is for one hand because of the higher polarization energy of some rotamers which were destabilized in the gas phase, and for other hand because of some interactions with medium make less important the group's orientation and the dipole of the molecule (Table 3).

All anionic species that keep the 3-OH group prefer to adopt nonplanar structures in the gas phase. These nonplanar structures show a distorted B-ring in response to the orientation of the 3-OH group, whose ω_1 and θ dihedral angles display, respectively, average values of 18.5 and 29.2°. The relative energies of planar structures vary from 2.0 kJ mol^{-1} (Pg) to 6.2 kJ mol^{-1} (Dp; Table 3). In contrast, planar structures are the most stable ones in solution by at least 8.0 kJ mol^{-1} (Figure 5).

As what found for the **N5** tautomer in Pn and Pt, the orientation of the 3′-methoxyl group has important consequences. In fact, the syn or anti orientation of this group in **A35** involves a variation of 22.8 kJ mol^{-1} in Pn. This energy change can be explained as a consequence of the different strength of the IHBs formed in both cases: O4′−H4′···O3′ for the syn orientation of ω_4 and ω_5 and C3′−H3′···O4′ for the corresponding anti orientation. The former orientation yields planar conformers, whereas the latter provides nonplanar ones. However, contrary to what is found for **N4′** (Table 3), the most stable rotamer of the **A54′** anion of Pn and Pt, display a slight preference (2.5 and 3.1 kJ mol^{-1}, respectively) for the anti orientation of the methoxyl group attached to C3′ in the gas phase. Nevertheless, PCM keeps the preferences for the syn by more than 5 kJ mol^{-1}.

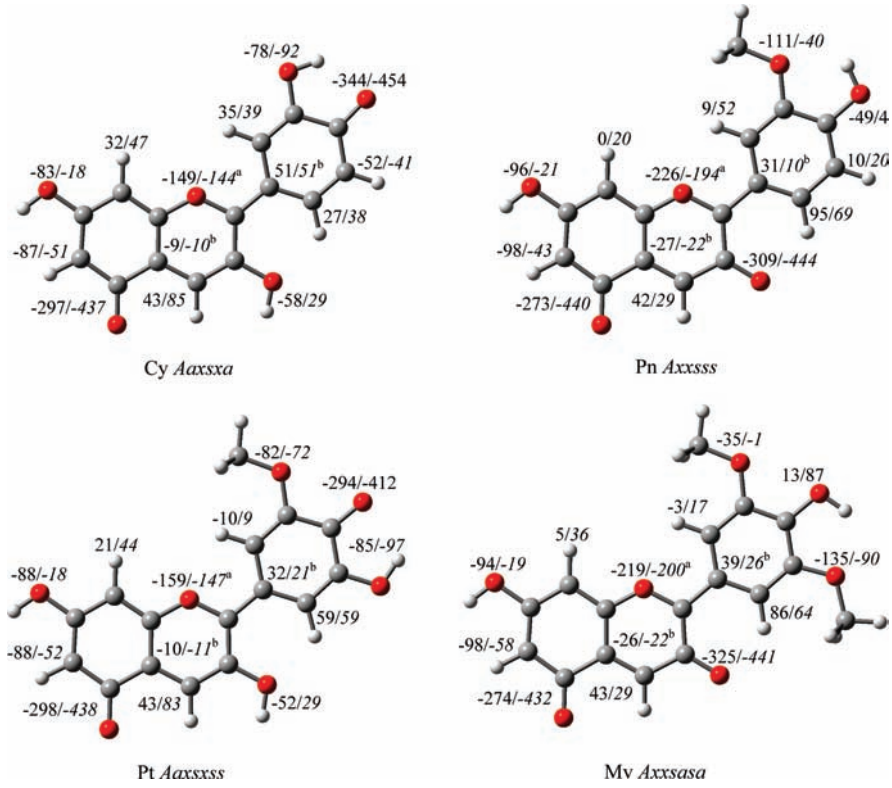

Figure 5. Most stable planar rotamer for the most stable tautomer of anionic Cy, Pn, Pt, and Mv in the gas phase. QTAIM charges (in au multiplied by 10^3) summed up into groups are shown for the gas phase and aqueous solution (in italics).

Second deprotonation also gives rise to some variations in the bond lengths of the polycyclic system. Comparing the most stable rotamer of the neutral (**N4′** or **N5**) and anion forms (**A35** and **A54′**), we observe changes in the bond lengths of the whole AC-B system. The main differences between **N4′** and **A54′** tautomers are those observed in the A ring (C5−C10 and C5−C6 lengthen), but important changes are also observed in C (C4−C10 shrinks) and in B systems (C4′−O4′ lengthens 0.022 Å). When the most stable tautomers are **N5** and **A54′**, the main differences are observed in B and C rings (C1′−C2′, C1′−C5′, C3′−C4′, and C4′−C5′ lengthen, C2−C1′, C4′−O4′, and C3−C4 shrink).

The C−O bond lengths of deprotonated hydroxyls are different. Two cases can be distinguished: (i) In **A54′**, the C4′−O4′ bond lengths are larger (1.267 Å in Cy and 1.277 Å in Dp) or equal (1.278 Å Pt) than the C5−O5 ones (1.259 Å for Cy and Dp) in those anthocyanidins with an ortho hydroxyl in the B-ring, but shorter (1.250 and 1.260 Å, respectively) when this hydroxyl is not present (Pg, Pn, and Mv); (ii) In contrast, we observe that the C5−O5 (1.253 Å) is always shorter than the C3−O3 bond length (1.270 Å) in **A35** anions (Table 2). This fact could be employed to analyze which of the two Lewis structures (leaving the negative charge on one of the different deprotonated hydroxyls) is preferred by each anthocyanidin. Nevertheless, we have to warn on the unreliability of assigning negative charges to atoms on the exclusive basis of geometrical features.[16] Thus, we have obtained integrated QTAIM atomic charges pointing to a more realistic description of negative charge distribution (see below).

Comparing solution and gas phase geometries, we observe a general increase of C−C bond lengths, except those involving a carbon attached to deprotonated oxygens. The O3···H6′−C6′ IHB is also detected as a bond path in the anions in both phases. Interatomic distances and ρ_b values indicate deprotonation weakens this IHB in **A54′** anions with regard to the corresponding neutral tautomers. This trend reverses for **A35** in which the IHB is stronger than in **N3** or **N5**. **A54′** tautomers also display other IHBs detected as a bond path between O4′ and the hydrogen of the adjacent hydroxyl group as in the **N4′** forms of Cy, Dp, and Pt. Shorter interatomic distances and larger ρ_b values indicate this IHB is stronger in **A54′** than in **N4′**. The BCP properties of the H4′···O3′ and H4′···O5′ IHB in **A35** show this interaction is stronger in Mv (Supporting Information). As commented for previous forms, bond paths among the substituents of the B ring are not detected with PCM electron densities.

Equilibria Among the Main Protrotropic Forms. Figure 6 summarizes main structural evolution of anthocyanidin due to protonation equilibria according to our B3LYP/6-31++G** conformational analysis and the corresponding Boltzmann distribution functions.[34] Structures shown in this figure represents at least 20% of the conformational equilibrium mixture at 298 K for each anthocyanidin form. Each tautomer indicated encompasses the equilibrium population of the diverse rotamers shown in Tables 1 and 3. pK_as (Table 4) are obtained according to conformationally averaged protonation dissociation energies (PDEs) in terms of *G*. Thus, average values of *G* are obtained for cations, neutral, and anions of each of the six anthocyanidins. Only relative pK_as, referred to phenol, are shown in Table 4 because of the problems affecting chemical accuracy of absolute pK_a values.[35]

Thus, looking at Figure 6, for example, we notice that when pH equals the first pK_a of Dp, we should find a mixture of the **N4′** neutral form and *Cas*---- cations for an aqueous solution of Dp, but exclusively cationic forms for aqueous solutions of any other anthocyanidin. Between the first pK_a of Pn and the second pK_a of Pt, neutral species of the six anthocyanidins should be the most populated forms in aqueous solution. **N4′**

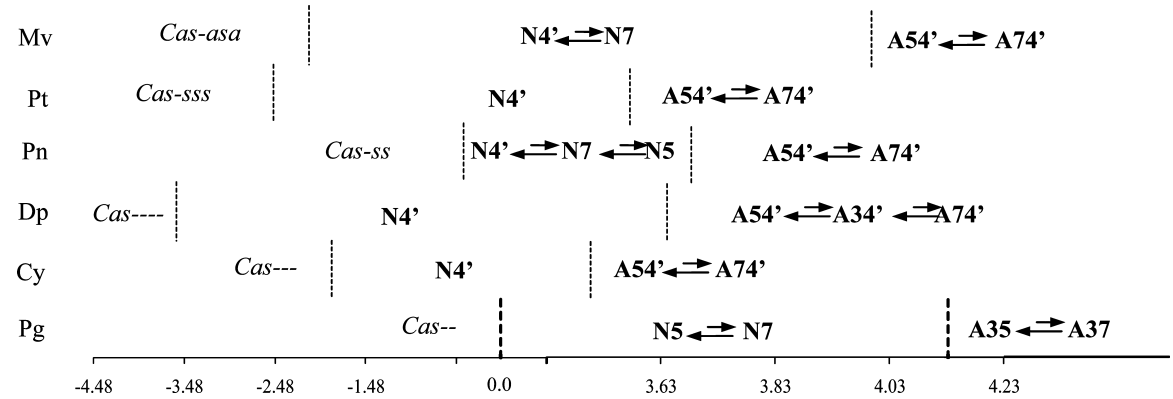

Figure 6. Most significant species (only those where Boltzmann population exceeds 20%) in aqueous solution at 298 K. *x*-Axis scale represents relative values of pK_a with regard to the first one of Pg (see Table 4).

TABLE 4: Relative pK_a Values at 298.15 K (with Regard to Phenol) Corresponding to the First, pK_{a1}, and Second, pK_{a2}, Deprotonations in the Acid/Base Equilibria for each Anthocyanidin

	ΔpK_{a1}[a] (C↔N)	ΔpK_{a2}[a] (N↔A)
Pg	−9.57	−5.44
Cy	−11.43	−6.07
Dp	−14.23	−5.93
Pn	−9.99	−5.89
Pt	−12.07	−5.94
Mv	−10.86	−5.56

[a] Relative to phenol (ΔG = 303.95 kcal mol^{-1}).

being the most populated tautomer in all cases but for Pg. Finally, rising pH above the second pK_a of Pg, only anionic forms should be present. **A54′** is the most favored one, with a significant contribution of **A74′** (and **A34′** in Dp), if we exclude the case of Pg, where **A35** is the most favored one with a significant contribution of **A37**.

QTAIM Electron Density Analysis. This analysis allows us to clarify (i) the distribution of the positive charge on the cations and that of the negative charge on the anions; (ii) the enolate or quinonoidal character of neutral forms; (iii) the most suitable position for the formal C═O double bond in the resonance forms written for the anions; (iv) the effects of substitution and conformational changes on the electron distribution; and (v) how solvent effects affect the electron distribution.

(i) Electron Distribution in Charged Species. The summation of the electron atomic charge of the atoms of the B-ring and those of the AC system shows that, for all the anthocyanidins, the positive charge of the cationic forms is spread throughout the whole molecule. Thus, over 44% of the charge is in the B-ring (Figure 2). We also notice that more than 30% of total positive charge is at the hydrogens (Table 5).

As previously observed for flavylium and pelargonidin cations,[12] it is not possible to localize the positive charge on a specific atom or set of atoms. Thus, the commonly drawn Lewis structures for these cations, in which the positive charge is usually located at O1 or C2, are not supported by QTAIM results. O1, far from bearing a positive charge, displays a significant negative one, and even summing the atomic population of atoms C2, O1, and C9 (hereafter we refer to it as α group) we found a negative formal charge. Even if we look at the relative electron population of the α group in the cations with regard to the neutral forms (Table 5), we notice a very small decrease of its negative charge. In fact, $\Delta q(\alpha)$ varies between 0.063 and 0.075 au in gas phase along the series of anthocyanidins and between 0.065 and 0.088 au with PCM. In contrast, the largest increases of positive charge upon protonation of neutral forms are obtained for the C−O group which receives the proton and for the whole B ring (even when the protonation site is located on the AC system Δq(B) exceeds 0.240 au in gas phase or 0.100 au in PCM).

Furthermore, looking at $q(\Omega)$ values,[36] we observe that there are some atoms that are not in line with the predictions of the resonance model (RM). According to it, we should also find a positive charge at C4, C5, C7, C2′, C4′, or C6′, but not at C8 or C6. Nevertheless, q(C8) and q(C6) are almost equal to q(C4) and higher than q(C6′) or q(C2′). Also, q(C1′) (which should not display positive charge according to the RM) is larger than q(C4).

For the anions, QTAIM analysis indicates the negative charge is mainly spread among three regions of the molecule (Figure 5): the two C−O units where hydrogens have been removed (averages are −0.277 au for C5−O5, −0.275 au for C4′−O4′, and −0.317 au for C3−O3) and the α area, which varies from −0.146 to −0.226 au. Relative charges, with regard to the corresponding neutral forms, indicate that more than 40% (more than 50% with PCM) of the charge involved in the deprotonation process is taken from deprotonated C−O units (Table 5). That is, these groups act as electron density sinks. Also, the rest of the hydrogens receive a significant amount of electron density (from 0.079 to 0.200 au) although most of them keep $q(\Omega)$ positive values. Finally, the electron density gained by the α region represents in all cases less than 5%.

Overall, as previously reported by Slee and MacDougall for allyl ions[37] QTAIM net charges are not in accord with RM expectations and predictions based on simple π-orbital models.

(ii) Enolate Versus Quinonoidal Character of Neutral Species. The usually represented quinonoidal Lewis structure containing a C═O double bond for representing the neutral form of anthocyanidins (Figure 4) is mainly supported, as commented above, by the comparison of bond lengths between the most stable neutral and cationic rotamers. Nevertheless, several resonance structures displaying positive and negative sites, enolate-like structures, can also be drawn for neutral anthocyanidins (Figure 4). Taking into account previously observed shortcomings when resonance structures are employed for qualitative descriptions of electron distributions, we think that the electron distribution of neutral anthocyanidins species should be analyzed with some detail before accepting they bear a quinonoidal structure.

As a general rule, we observe that electroneutrality is obtained by compensation of substantially negatively charged areas (α group and deprotonated CO) and the rest of the molecule, where all the atoms (if we exclude exceptions like the CH at 6 in **N5**

TABLE 5: QTAIM Atomic Charges Summed up into Groups (in au) for Selected Structures of the Cationic, Neutral, and Anionic Forms of the Six Anthocyanidins

		$q_{(\text{B-ring})}$ gas/PCM	$q_{(\alpha)}$ gas/PCM	$q_{(\text{H})}$[a] gas/PCM	$q_{(\text{COH})}/q_{(\text{CO})}$[b] gas/PCM
cationic forms[c]	Pg	0.448/0.362	−0.048/−0.036	0.437/0.565	0.072/0.089
	Cy	0.438/0.359	−0.044/−0.038	0.393/0.512	0.036/0.051
	Dp	0.445/0.349	−0.042/−0.035	0.347/0.455	0.088/0.063
	Pn	0.482/0.361	−0.059/−0.041	0.391/0.492	0.067/0.070
	Pt	0.465/0.378	−0.054/−0.038	0.343/0.466	0.068/0.073
	Mv	0.506/0.356	−0.058/−0.039	0.315/0.423	0.063/0.103
neutral forms[c]	Pg	0.205/0.239	−0.120/−0.124	0.280/0.434	−0.207/−0.381
	Cy	−0.085/−0.345	−0.119/−0.103	0.230/0.394	−0.236/−0.397
	Dp	−0.097/−0.346	−0.116/−0.101	0.221/0.371	−0.277/−0.393
	Pn	0.209/−0.321	−0.126/−0.109	0.268/0.365	−0.208/−0.351
	Pt	0.203/−0.327	−0.123/−0.107	0.253/0.364	−0.206/−0.350
	Mv	0.225/−0.294	−0.121/−0.115	0.230/0.332	−0.210/−0.302
anionic forms[d]	Pg	−0.368/−0.499	−0.156/−0.145	0.080/0.289	−0.300/−0.437//−0.287/−0.458
	Cy	−0.391/−0.510	−0.149/−0.144	0.111/0.285	−0.344/−0.454//−0.297/−0.437
	Dp	−0.414/−0.510	−0.146/−0.141	0.142/0.277	−0.389/−0.454//−0.292/−0.434
	Pn	−0.383/−0.503	−0.151/−0.143	0.113/0.287	−0.289/−0.419//−0.298/−0.437
	Pt	−0.381/−0.493	−0.159/−0.147	0.116/0.256	−0.298/−0.412//−0.294/−0.438
	Mv	−0.323/−0.458	−0.164/−0.152	0.095/0.244	−0.305/−0.445//−0.184/−0.362

[a] Values refer to the sum of the formal charge of the hydrogens attach to C sp^2. [b] In cations these values refer to the formal charge of the COH group, which is the most favored site to deprotonate; in neutral tautomers these values are referred to the formal charge of the CO, which is deprotonated; and in the anions they are referred to the formal charge of the two CO units, which are deprotonated in the order: q(CO5) in the gas phase/q(CO5) in solution//q(CO4′) in the gas phase/q(CO4′) in solution. [c] Values refer to the global formal charge obtained summing into groups for the most stable rotamer of cationic form of the six anthocyanidins and the most stable neutral tautomer in each phase (see Tables 1 and 3). [d] Values refer to the most stable rotamer of **A54′** tautomer for the six anthocyanidins in both phases, although, in some cases, it is not the most stable one.

tautomers) bear moderate positive charges. It should be remarked that the charge of the deprotonated CO unit (CO^{dep}) is, in all molecules and tautomers, more negative than −0.206 au. Thus, looking at the most stable tautomers, we observe (Figure 3) the C4′−O4′ bond displays negative charge (−0.236 au) in the **N4′** tautomer of Cy, whereas the corresponding COH group in the cation (Figure 2) is slightly positive (0.036 au) as it has been obtained for the **N4′** tautomer of Dp (−0.277 au and 0.086 au, respectively).[16] The same pattern is observed in **N5** for the remaining anthocyanidins. Thus, we find the C5−O5 bond goes from a slightly positive charge in the cations (0.063 to 0.068 au) to a negative charge (−0.206 to −0.210 au) in the neutral tautomer. In general, $q(CO^{dep})$ is more negative than those found for a carbonyl group in aliphatic systems[38] in spite of there being less surrounding hydrogens (the atoms that act as electron donors) in anthocyanidins than in aliphatic aldehydes and ketones. Although this could point to a significant weight of the enolate forms, we do not observe the accompanying set of positive charges predicted by RM at C2, C4, C5, C7, C9, C2′, C4′, and C6′, and neutral charges at C3, C6, C8, C10, C1′, C3′, and C5′. Clearly, some QTAIM atomic charges are not in line with this rule, for example, q(C1′) > q(C2′), q(C10) > q(C4), and so on. Overall, QTAIM results indicate that, in spite of their geometry, neutral forms display a certain enolate character, bearing a negative charge around the deprotonated oxygen but counterbalanced in a different fashion than that expected from the typically enolate-like resonance structures.

As commented above, **N3** tautomer cannot be graphed without implying formal charges. Rastelli et al.[13] argued that this fact causes its high relative energies. Nevertheless, we have found that **N3** is not the highest energetic tautomer; even for Mv, it is only 3.1 kJ mol^{-1} above the minimum in the gas phase. One "contributing structure" for **N3** tautomers, shown in Figure 4 and reported by Rastelli, places a partial positive charge on O1 and a partial negative charge on O3. Analyzing the atomic electron density of **N3**, we find that q(O1) is even more negative than in the most stable tautomer, **N5**. We also find a significant negative charge on 4-CH, 5′-$COCH_3$, and on the α group (−0.039, −0.028, and −0.142 au, respectively). Significant positive charges are found in 8-CH and 6′-CH groups. The existence of **N3** could be taken as a further indication that neutral forms of anthocyanidins are closer to enolate-like more than to quinonoidal structures.

(iii) Location of the Formal C═O Double Bond in Anions. Geometrical trends point to a preference for locating this bond on C5═O5 in **A35** tautomers of all molecules and in **A54′** ones of Cy and Dp. According to these trends it will locate on C4′═O4′ in **A54′** of Pg, Pn, and Mv (those where there is no ortho hydroxyl in the B-ring). Finally, C5−O5 and C4′−O4′ bond distances are equivalent in *Pt*-**A54′**. These geometrical features are confirmed by QTAIM charges of the most stable anionic tautomers in gas and solution phases (Table 5 and Figure 5). Thus, in **A35** tautomers q(C3) + q(O3) is always more negative than q(C5) + q(O5), favoring the location of the enolate unit on C3−O3 and the double bond on C5═O5, in agreement with the impossibility of writing isovalent resonance structures for anthocyanidins when a double bond is drawn between C3 and O3. This can be observed in the most stable tautomers of Pn and Mv (gas phase) and Pg (solution). For **A54′** tautomers we can distinguish three cases: (a) $|q(C4') + q(O4')| > |q(C5) + q(O5)|$ in Dp and Cy; (b) $|q(C4') + q(O4')| = |q(C5) + q(O5)|$ in Pt; and (c) $|q(C4') + q(O4')| < |q(C5) + q(O5)|$ in Pg, Pn, and Mv. Obviously, case (a) favors the location of the double bond on C5═O5, case (c) on C4′═O4′, and case (b) suggests the equivalence between both structures.

(iv) Effects of Substitution and Conformational Changes on the Electron Distribution. The series of anthocyanidins can be presented as obtained by progressive substitutions of a common Pg structure, where hydrogens which are ortho to 4′-OH are replaced by -OH and -OCH_3 groups. We notice that there are not simple general rules for modifications of electron distribution upon these substitutions. Thus, the electron population of the B-ring may be increased or decreased (with regard to that of Pg) by adding the same set of substituents depending

on the global charge of the molecule (C, N, or A forms; Table 5). The only general rule we observe is that replacement of -OH by -OCH_3 groups decreases the total electron population of the B-ring. This can be noticed both in the Dp, Pt, Mv or in the Cy, Pn series, even in spite of the different tautomers involved in this comparison for **N** forms. Similarly, the electron population of the α-region increases slightly upon replacement of -OH by -OCH_3 if we exclude the neutral forms of Pt and Mv.

The main effects of conformational changes originated by the orientation of 3-OH, 5-OH, and 7-OH have been already discussed for Pg in a previous paper and should remain nearly constant in these systems. Therefore, we concentrate on the effects caused by the orientation of the B-ring substituents. There are two significant ones: (a) q(4′-COH) decreases when this group is involved as H-acceptor and increases when it acts as H-donor in IHB with neighboring groups; and (b) the positive charge of the neighboring CH groups of the substituents is depleted or enhanced depending, respectively, if the H and the substituent are placed in the molecular plane at the same or opposite sides of the line defined by the latter's C−O bond.

(v) Solvent Effects on the Electron Distribution. In general, as could be expected, PCM electron densities enlarge (with regard to the gas phase) the absolute values of atomic charges in the periphery of the molecule. This is observed in all the species. Thus, in cations, PCM indicates that solvation decreases the negative charge in the α-group and the positive charge at the whole B-ring (lower than 38%), but the positive charge of hydrogens increases totaling 42−56% of the global charge.

Changes in neutral species can be summarized as electron density transference from the AC system to the hydrophilic part of B-ring in **N4′**. Also, in contrast with the gas phase, the C−O−H units become significantly charged (they are negative in B and positive in AC). We also observe that q(O4′) and q(O5) are substantially larger in PCM than in the gas phase, whereas the reverse trend is observed for q(C2), which could be interpreted as the PCM electron distribution enhances the weight of enolate-like forms, while q(O1) keeps nearly constant.

In anions, the main difference found between group charges in PCM and gas phase is the enlargement of the electron density of the deprotonated hydroxyls, whose negative charges represent more than 88% of the molecular one. This electron density is taken from the rest of the molecule with no noteworthy exception.

Conclusions

The results of a detailed DFT study on the acid/base, prototropic, and conformational equilibria of anthocyanidins in gas phase and PCM modeled aqueous solution indicate that, excluding pelargonidin, the most favored neutral tautomers in solution are deprotonated at C4′. With the same exception, deprotonations at C5 and C4′ characterize the most stable anionic tautomers in solution. The equilibrium population of tautomers is mainly modified along the series by the substitution pattern on the B-ring. QTAIM electron density analysis show that the electron distribution of cations, neutral forms, and anions is not well described by the Lewis structures usually employed to represent them. Thus, in cations, the positive charge is spread throughout the whole molecule and it is not possible to localize the positive charge on a specific atom or set of atoms. For the anions, the negative charge is mainly spread among three regions of the molecule: the two C−O units where hydrogens have been removed and the α area. The usually represented quinonoidal Lewis structure containing a C=O double bond for representing the neutral form of anthocyanidins is mainly supported by the comparison of bond lengths between the most stable neutral and cationic rotamers. Nevertheless, we observe that electroneutrality is obtained by compensation of substantially negatively charged areas (α group and deprotonated CO) and the rest of the molecule, where all the atoms bear moderate positive charges, pointing to a significant weight of the enolate forms bearing a negative charge around the deprotonated oxygen but counterbalanced in a different fashion than that expected from the typically enolate-like resonance structures. Geometrical trends and QTAIM charges point to a preference for locating a double bond on C5=O5 in **A35** tautomers of all molecules and in **A54′** ones of Cy and Dp. In general, as could be expected, PCM electron densities enlarge (with regard to the gas phase) the absolute values of atomic charges in the periphery of the molecule. Thus, in cations, PCM indicates that solvation decreases the negative charge in the α group and the positive charge at the whole B-ring, but the positive charge of hydrogens increases totaling 42−56% of the global charge. In neutral species we notice the PCM description transfers electron density from the AC system to the hydrophilic part of B-ring in **N4′**. In anions, the main difference is the enlargement of the electron density of the deprotonated hydroxyls.

Acknowledgment. L.E. thanks Universidade de Vigo for a predoctoral fellowship. Authors thank "Centro de Supercomputación de Galicia" (CESGA) for free access to its computational facilities and Spanish MEC for funding this research through Project CTQ2006-15500.

Supporting Information Available: Bond lengths, angles, and vibrational frequencies. This material is available free of charge via the Internet at http://pubs.acs.org.

References and Notes

(1) Francis, F. Color in food. In *Color in Food: Improving Quality*; MacDougall, D. B., Ed.; CRC Press: Boca Raton, FL, 2002; p 297.
(2) Kalt, W.; McDonald, J. E.; Ricker, R. D.; Lu, X. *Can. J. Plant Sci.* **1999**, *79*, 617.
(3) Mazza, G.; Brouillard, R. *Food Chem.* **1987**, *25*, 207.
(4) Nielsen, S. R.; Holst, S. Color in food. In *Color in Food: Improving Quality*; MacDougall, D. B., Ed.; CRC Press: Boca Raton, FL, 2002; p 331.
(5) Mishira, D. K.; Dolan, K. D.; Yang, L. *J. Food Sci.* **2008**, *73*, 9.
(6) Heredia, F. J.; Franchia-Aricha, E. M.; Rivas-Gonzalo, J. C.; Vicario, I. M.; Santos-Buelga, C. *Food Chem.* **1998**, *63*, 491.
(7) Brouillard, R. In *Anthocyanins as Food Colors*; Markasis, P., Eds.; Academic Press: New York, 1982; p 1.
(8) Andersen, O. M. In *Encyclopedia of Life Sciences*; MacMillan Publishers Ltd.: London, 2002; p 597.
(9) Sakakibara, H.; Ashida, H.; Kanazawa, K. *Free Radical Res.* **2002**, *36*, 307.
(10) Woodford, J. N. *Chem. Phys. Lett.* **2005**, *410*, 182.
(11) Sakata, K.; Saito, N.; Honda, T. *Tetrahedron* **2006**, *62*, 3721.
(12) Estévez, L.; Mosquera, R. A. *Chem. Phys. Lett.* **2008**, *451*, 121.
(13) Rastelli, G.; Costantino, L.; Albasini, A. *J. Mol. Struct.: THEOCHEM* **1993**, *279*, 157.
(14) Borkowski, T.; Szymusiak, H.; Gliszczynska-Swiglo, A.; Rietjens, I. M. C. M.; Tyrakowska, B. *J. Agric. Food Chem.* **2005**, *53*, 5526.
(15) Estévez, L.; Mosquera, R. A. *J. Phys. Chem. A* **2007**, *111*, 11100.
(16) Estévez, L.; Mosquera, R. A. *J. Phys. Chem. A* **2008**, *112*, 10614.
(17) Miertu, S.; Scrocco, E.; Tomasi, *J. Chem. Phys.* **1981**, *55*, 117.
(18) Cossi, M.; Barone, V.; Cammi, R.; Tomasi, J. *Chem. Phys. Lett.* **1996**, *255*, 327.
(19) (a) Vila, A.; Mosquera, R. A. *J. Phys. Chem. A* **2000**, *104*, 12006. (b) Vila, A.; Mosquera, R. A. *Chem. Phys. Lett.* **2000**, *332*, 474. (c) González-Moa, M. J.; Mosquera, R. A. *J. Phys. Chem. A* **2003**, *107*, 5361. (d) González-Moa, M. J.; Mosquera, R. A. *J. Phys. Chem. A* **2005**, *109*, 3682. (e) González-Moa, M. J.; Mosquera, R. A. *J. Phys. Chem. A* **2006**, *110*, 5934. (f) Otero, N.; González Moa, M. J.; Mandado, M.; Mosquera, R. A. *Chem. Phys. Lett.* **2006**, *428*, 249.

(20) (a) Bader, R. F. W. *Chem. Rev.* **1991**, *91*, 893. (b) Bader, R. F. W. In *Atoms in Molecules: A Quantum Theory*; Oxford University Press: New York, 1990.

(21) Matta, C.; Boyd, R. J. The Quantum Theory of Atoms in Molecules. *Solid State to DNA and Drug Design*; Wiley-VCH: Weinheim, 2007.

(22) Popelier, P. L. A. *Atoms in Molecules. An Introduction*; Prentice Hall: Harlow, 2000.

(23) Bader, R. F. W. *Monatsh. Chem.* **2005**, *136*, 819–854.

(24) (a) Becke, A. D. *J. Chem. Phys.* **1993**, *98*, 5648. (b) Lee, C.; Yang, G.; Parr, R. G. *Phys. Rev.* **1988**, *37*, 785.

(25) Frisch, M. J.; Trucks, G. W.; Schlegel, H. B.; Scuseria, G. E.; Robb, M. A.; Cheeseman, J. R.; Montgomery, J. A., Jr.; Vreven, T.; Kudin, K. N.; Burant, J. C.; Millam, J. M.; Iyengar, S. S.; Tomasi, J.; Barone, V.; Mennucci, B.; Cossi, M.; Scalmani, G.; Rega, N.; Petersson, G. A.; Nakatsuji, H.; Hada, M.; Ehara, M.; Toyota, K.; Fukuda, R.; Hasegawa, J.; Ishida, M.; Nakajima, T.; Honda, Y.; Kitao, O.; Nakai, H.; Klene, M.; Li, X.; Knox, J. E.; Hratchian, H. P.; Cross, J. B.; Bakken, V.; Adamo, C.; Jaramillo, J.; Gomperts, R.; Stratmann, R. E.; Yazyev, O.; Austin, A. J.; Cammi, R.; Pomelli, C.; Ochterski, J. W.; Ayala, P. Y.; Morokuma, K.; Voth, G. A.; Salvador, P.; Dannenberg, J. J.; Zakrzewski, V. G.; Dapprich, S.; Daniels, A. D.; Strain, M. C.; Farkas, O.; Malick, D. K.; Rabuck, A. D.; Raghavachari, K.; Foresman, J. B.; Ortiz, J. V.; Cui, Q.; Baboul, A. G.; Clifford, S.; Cioslowski, J.; Stefanov, B. B.; Liu, G.; Liashenko, A.; Piskorz, P.; Komaromi, I.; Martin, R. L.; Fox, D. J.; Keith, T.; Al-Laham, M. A.; Peng, C. Y.; Nanayakkara, A.; Challacombe, M.; Gill, P. M. W.; Johnson, B.; Chen, W.; Wong, M. W.; Gonzalez, C.;and Pople, J. A. *Gaussian 03*, Revision E.01; Gaussian, Inc.: Wallingford, CT, 2004.

(26) Tomasi, J.; Mennuci, B.; Cammi, R. *Chem. Rev.* **2005**, *105*−2999.

(27) Bader, R. F. W. *AIMPAC: A Suite of Programs for the Theory of Atoms in Molecules*; McMaster University: Hamilton, Ontario, Canada, 1994.

(28) Bader, R. F. W. *J. Phys. Chem. A* **1998**, *102*, 7314–7323.

(29) Gillespie, R. J.; Popelier, P. L. A. *Chemical Bonding and Molecular Geometry: From Lewis to Electron Densities*; Oxford University Press: New York, 2001.

(30) $\upsilon_{(C6'-H6')}$ decreases by more than 30 cm^{-1} (3265.6 cm^{-1}) and $r_{(C6'-H6')}$ increases (1.080 Å) in the rotamer Pt *Casaaaa* with regard to *Casasss* ($\upsilon_{(C6'-H6')}$ = 3296.1 cm^{-1}, $r_{(C6'-H6')}$ = 1.078 Å). This indicates a shift towards red shifted IHB in the former. The same trend, although with a slighter effect, was found in Pn *Casaaa* ($\upsilon_{(C6'-H6')}$ = 3287.4 cm^{-1}, $r_{(C6'-H6')}$ = 1.079 Å) versus Pn *Casass* ($\upsilon_{(C6'-H6')}$ = 3294.8 cm^{-1}, $r_{(C6'-H6')}$ = 1.078 Å) and in Mv *Casasss* ($\upsilon_{(C6'-H6')}$ = 3295.9 cm^{-1}, $r_{(C6'-H6')}$ = 1.078 Å) versus *Casaasa* ($\upsilon_{(C6'-H6')}$ = 3306.0 cm^{-1}, $r_{(C6'-H6')}$ = 1.077 Å).

(31) (a) Klein, R. A. *J. Am. Chem. Soc.* **2002**, *124*, 13931. (b) Klein, R. A. *J. Comput. Chem.* **2002**, *23*, 585. (c) Mandado, M.; Graña, A. M.; Mosquera, R. A. *Phys. Chem. Chem. Phys.* **2004**, *6*, 4391. (d) Mandado, M.; Mosquera, R. A.; Van Alsenoy, C. *Tetrahedron* **2006**, *62*, 4243.

(32) Leopoldini, M.; Russo, N.; Toscano, M. *J. Agric. Food Chem.* **2006**, *54*, 3078.

(33) Klamt A. Communication to the Computational Chemistry List, http://www.ccl.net/htdig.

(34) Mac Quarrie, D. *Statistical Mechanics*; University Science Books: Sausalito, 2000.

(35) Liptak, M. D.; Shields, G. C. *Int. J. Quantum Chem.* **2001**, *85*, 727.

(36) Complete tables of QTAIM charges may be obtained from the authors upon request.

(37) Slee, T. S.; MacDougall, P. J. *Can. J. Chem.* **1988**, *66*, 2961.

(38) Graña, A. M.; Mosquera, R. A. *J. Chem. Phys.* **1999**, *110*, 6606.

JP904298Z